Fluorescence Lifetime Imaging Microscopy for the Detection of Intracellular pH with Quantum Dot Nanosensors

ARTICLE *in* ACS NANO · JUNE 2013

Impact Factor: 12.88 · DOI: 10.1021/nn402581q · Source: PubMed

3 AUTHORS:

Angel Orte
University of Granada
66 PUBLICATIONS **1,189** CITATIONS
SEE PROFILE

Jose M Alvarez-Pez
University of Granada
63 PUBLICATIONS **920** CITATIONS
SEE PROFILE

Maria J Ruedas-Rama
University of Granada
38 PUBLICATIONS **689** CITATIONS
SEE PROFILE

Fluorescence Lifetime Imaging Microscopy for the Detection of Intracellular pH with Quantum Dot Nanosensors

Angel Orte, Jose M. Alvarez-Pez, and Maria J. Ruedas-Rama*

Department of Physical Chemistry, Faculty of Pharmacy, University of Granada, Campus Cartuja, 18071, Granada, Spain

ABSTRACT While the use of quantum dot (QD) nanoparticles for bioimaging and sensing has been improved and exploited during the last several years, most studies have used emission intensity-based techniques. Fluorescence lifetime imaging microscopy (FLIM) can also be employed for sensing purposes, overcoming many of the limitations of the aforementioned systems. Herein, we show that the photoluminescence (PL) lifetime of mercaptopropionic acid-capped QDs (MPA-QDs) collected from FLIM images can be used to determine intracellular pH. The PL average lifetime of MPA-QDs varied from 8.7 ns (pH < 5) to 15.4 ns (pH > 8) in media mimicking the intracellular environment. These long decay times of QD nanoparticles make them easily distinguishable from intrinsic cell autofluorescence, improving selectivity in sensing applications. We demonstrate, for the first time, the successful detection of changes in the intracellular pH of different cell types by examining the PL decay time of QDs. In particular, the combination of FLIM methodologies with QD nanoparticles exhibits greatly improved sensitivity compared with other fluorescent dyes for pH imaging. A detailed description of the advantages of the FLIM technique is presented.

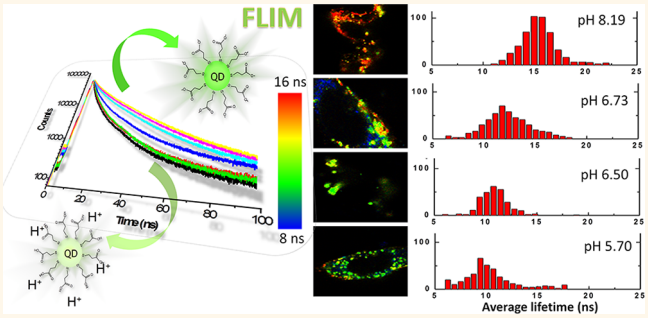

KEYWORDS: fluorescence lifetime imaging microscopy · quantum dot · pH nanosensor · intracellular sensing

Semiconductor nanocrystals or quantum dots (QDs) are established photoluminescent (PL) platforms for biological and sensing applications. QDs feature high quantum yield, resistance to photobleaching, photostability, broad absorption spectra, narrow photoluminescence spectra, and size-tunable emissions. These optical properties suggest that they are ideally suited for long-term monitoring of intracellular processes.[1] In recent years, new strategies for sensing using QDs have emerged. Most of the proposed QD nanoparticle sensors are based on the enhancement or quenching of the PL emission intensity upon reaction or interaction with the target analyte.[2−4] However, fluorescence intensity-based measurements suffer from uncertainties in the calibration of the responses, particularly when those systems are applied as intracellular probes. For example, the emission intensity can be altered by the fluctuations in the probe concentration and heterogeneities in the optical properties of the medium. Furthermore, the relative localization of the nanosensor in certain compartments of the cell can produce misleading readouts.

The use of time-resolved fluorescence spectroscopy can overcome many of these limitations. The combination of this technique with QD nanoparticles is of particular interest because the PL average lifetime of QDs is significantly longer than that of most organic dyes (1−5 ns) and cell autofluorescence (2−3 ns) but is efficient enough to maintain a high photon stream.[5] These features indicate that the use of QDs as time-resolved PL nanosensors has great potential for multiplexing and time-gated cellular detection with enhanced selectivity and sensitivity. When using QDs as intracellular probes, fluorescence lifetime imaging microscopy (FLIM) can be a very effective technique for quantitative real-time sensing

* Address correspondence to mjruedas@ugr.es.

Received for review May 22, 2013 and accepted June 25, 2013.

Published online June 25, 2013
10.1021/nn402581q

of biologically important targets inside living cells. Note that although it would be more appropriate using the term "PL decay time", we will use instead PL lifetime for consistency with the name of the technique "fluorescence lifetime imaging microscopy".

In addition to long lifetimes (typically 5 to hundreds of nanoseconds), QDs also exhibit multiexponential PL decays, with the excited-state lifetime of colloidal QDs being an optical property of QDs that is not yet well-understood. These PL decay kinetics are related to the radiative and nonradiative pathways that an exciton undergoes to achieve electron–hole recombination and can be modified by changes on the surface environment.[6] Although these complex PL kinetics might be considered a difficulty or disadvantage, they can be overcome with the use of appropriate experimental arrangements and data analysis strategies. We previously demonstrated that time-resolved fluorescence spectroscopy is a sensitive technique that can be successfully applied to the detection and quantification of several interactions between QDs and other molecules based on different response mechanisms, such as charge or electron transfer.[7−9] Our studies were the first to report that the PL average lifetime of QD-based nanosensors can permit the quantification of analytes such as chloride ions or protons (pH) in bulk solutions mimicking the intracellular environment. QDs have also been conjugated with organic dyes for the development of fluorescence resonance energy transfer (FRET) systems for sensing applications, which use the PL lifetime as an analytical signal.[10,11]

However, only a few fluorescent approaches have used FLIM as the detection technique for intracellular sensing, mainly with organic fluorophores and fluorescent proteins, and these approaches displayed low sensitivity.[12−16] The combination of FLIM with fluorescent nanoparticles has not yet been exploited. A few examples with gold nanoparticles[17] and QD nanoparticles[18−22] have been described but only for the detection and not the quantification of the target molecules. Herein, we propose the use of FLIM in combination with pH-sensitive CdSe/ZnS QD nanoparticles for sensing of intracellular pH. To the best of our knowledge, this is the first time that a sensor with these features has been proposed in the literature. First, we demonstrated the possibility of quantifying the pH value by analyzing the FLIM images of mercaptopropionic acid-capped QDs suspended in buffered solutions. We further extended the methodology to the detection of changes in the intracellular pH of different types of cells. Our goal in this work is to provide an overview of the great potential of FLIM for intracellular imaging and sensing that will establish a basis for the use of QD nanoparticles in fluorescence lifetime-based nanosensors. With the proper modification of the QD surface for the creation of new nanoscale, intracellular-sensitive probes, this methodology can be extended to the quantification of a wide range of ions and molecules inside cells.

RESULTS AND DISCUSSION

MPA-QDs Suspended on Glass Slides. In a previous work, we proposed the use of MPA-QD nanoparticles as a suitable pH sensor in time-resolved fluorometry.[8] In order to test the potential of this sensor in FLIM applications, MPA-QD nanoparticles were first suspended in Tris buffer solutions with different pH values and deposited on the surface of a microscope glass slide (see Supporting Information for details and Figure S1). The analysis of the PL decay traces of the overall FLIM images revealed the characteristic features of the temporal behavior of the QD's PL emission. The PL decay traces of MPA-QDs in solution deposited on glass slides exhibited multiexponential decay kinetics. From these first experiments, it is observed that the MPA-QD average lifetime obtained from FLIM images was enhanced as the pH of the environment increased. As previously described, the PL intensity of MPA-QDs is sensitive to the degree of protonation of the mercaptopropionic acid capping the surface.[3,23,24] At basic pH, the carboxylic acid is deprotonated, and a negatively charged shell appears on the surface of the QDs, which increases the confinement of the charge carrier in the semiconductor, resulting in a higher band gap energy, shorter emission wavelengths, and higher quantum yields.[25] This pH sensitivity has been observed previously in steady-state PL spectra and PL decay traces of MPA-QDs in buffered solutions at different pH values.[8,26] The PL intensity of these MPA-QDs displayed a typical S-shaped curve with respect to the pH value, with a linear increase within the physiological pH range. The calibration plot from buffered solutions is in good agreement with the plot obtained previously using a time-resolved fluorescence spectroscopy method with similar MPA-QDs in bulk aqueous solutions (see Supporting Information).[8]

Nevertheless, if the MPA-QDs are intended to be employed as intracellular nanosensors, the highly crowded intracellular environment can alter their response. One limitation of QDs as probes in live cells is the nonspecific adsorption of intracellular components and the formation of a "protein corona".[27−29] QDs bind nonspecifically *via* electrostatic interactions to various cellular proteins, reducing their ability to interact with their corresponding targets and decreasing signal-to-noise ratios.[30,31] Thus, we evaluated next the pH response of the proposed MPA-QD nanosensors in solutions mimicking the cellular cytoplasm. MPA-QDs were dissolved in buffer solutions with a composition similar to that of the intracellular environment (see Experimental Section for composition) and adjusted to different pH values (synthetic intracellular buffers, SIBs). The MPA-QDs suspended in SIBs were deposited on the surface of a microscope glass slide, and FLIM

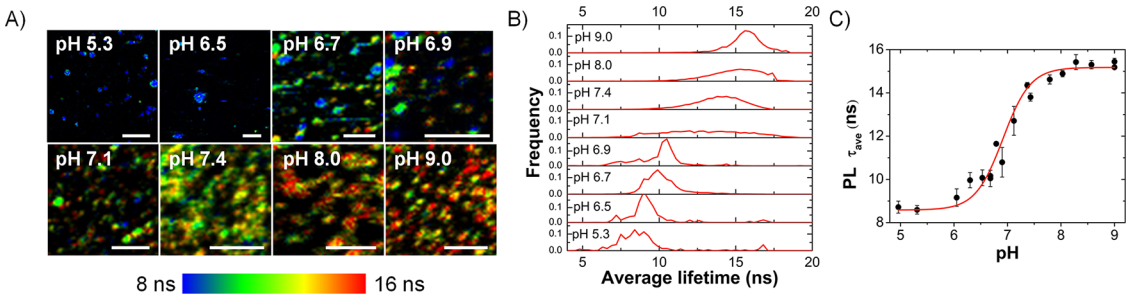

Figure 1. (A) FLIM images of MPA-QDs suspended in solutions mimicking the intracellular environment (SIB) at different pH values. The scale bars (white lines) represent 10 μm. (B) Examples of PL lifetime histograms collected from the images in (A). (C) pH response of MPA-QD nanosensors suspended in SIB based on data obtained from the FLIM images.

confocal images were recorded following the procedure and analysis described in the Experimental Section. The PL decays of MPA-QDs collected from the FLIM images exhibited multiexponential decay kinetics, and four exponential functions were needed to obtain the best fit. The analysis of the four-exponential decay traces of the MPA-QD PL in bulk solutions revealed that the calculated average lifetime was dependent on the pH value of the media, with a linear response in the physiological pH range.[8] In particular, of the four lifetime components of MPA-QD, only the two longest components decreased with decreasing pH because they are related to the surface states in recombination processes.[6] The shortest components were pH-independent, which can be attributed to the intrinsic recombination of populated core states.[32]

The FLIM technique allows the visual inspection of the spatial distributions of the PL lifetimes by analyzing the PL decay traces of the individual pixels. The average PL lifetimes in the individual pixels comprise the FLIM images depicted in Figure 1A. The arbitrary color scale clearly illustrates that the pH response of the proposed nanosensors was maintained, even in these crowded solutions, regardless of the presence of several ions, proteins, and polymers at relatively high concentrations. The frequency histograms of the average PL lifetime were obtained from the pixels of interest (those in which MPA-QDs were visible with a total intensity greater than a threshold value; see Methods) from several images (at least four) collected under the same conditions (Figure 1B). The inspection of these distributions also permits the establishment of the pH response of the nanosensor by looking at the shift in the populations. Finally, the arithmetic mean of the average lifetimes in the pixels of interest was obtained and plotted in Figure 1C. The PL average lifetime of MPA-QDs displayed an S-shaped variation similar to that observed with increasing pH of the Tris buffer solution. However, the calculated linear response range from MPA-QDs in the SIBs was narrower and shifted to higher pH values than that from MPA-QDs in Tris buffer. Under conditions mimicking intracellular media, the MPA-QDs responded linearly from pH 6 to 7.5. In addition, the average lifetimes at more acidic pH values were slightly higher, in agreement with passivation occurring at the surface as a result of the nonspecific adsorption of the proteins of the medium. The average lifetime of the nanosensors increased from 8.7 $\pm$ 0.3 ns (at pH < 5) to 15.4 $\pm$ 0.2 ns (at pH > 9) (Figure 1C). In this case, fewer free carboxylic groups are available to be protonated and produce changes in the PL signal. These variations in the response behavior are of particular interest when the nanosensors are applied to the quantification of pH in biological samples because the linear response is more closely centered on the physiological pH. Moreover, the standard error calculated for the average lifetime of MPA-QDs on a glass surface was consistently low, even though the PL lifetime distributions were calculated from several FLIM images, which indicates the robustness of the technique. We also compared the PL average lifetime of MPA-QDs suspended in the SIBs obtained from the FLIM images with those determined by conventional time-resolved fluorometry measurements (see Figures 1C and S2). Both sets of results were in good agreement.

When evaluating the performance of our proposed MPA-QD nanosensor, it is important to note that its sensitivity was higher than other types of fluorescent pH probes that use the same detection technique.[12,13,33] For example, a whole family of fluorescent protein-based pH sensors has been reported for which the maximum change in the fluorescence lifetime along the response range was ~1.5 ns.[12,13] Herein, the change in the PL average lifetime of the MPA-QD nanosensors from the lowest to the highest point of the linear response range was approximately 7 ns. This change in the analytical signal is in agreement with other QD-based pH nanosensors that exhibit linear response ranges around physiological pH. For instance, the PL average lifetime of a QD−dopamine bioconjugate shifted from ~7 to ~2.5 ns along the pH response range (pH 6.5−10.0).[34] In another example, the PL average lifetime of a hybrid QD−near-infrared dye changed from 29 ns (pH < 7) to 12 ns (pH < 5), although it was insensitive around the physiological pH, indicating that a ratiometric strategy would be required for

quantitative pH measurements in cells and tissues.[10] In addition, the high sensitivity achieved when measuring the average lifetime of QD-based nanosensors differs more greatly than that of conventional organic fluorescent probes when intracellular imaging is employed. In most reported FLIM applications, small changes in the fluorescence lifetime of the corresponding dyes were observed,[15,33,35] with changes sometimes as small as one-hundredth of a nanosecond.[14] This finding demonstrates the high potential of the use of QD nanoparticles for sensitive intracellular sensing using FLIM methodologies. Therefore, the linear response range, which corresponds to the pH range within the cell, and the good agreement between both the bulk solution measurements and the microscopy results suggest the suitability of the proposed MPA-QD nanosensors for pH determination in intracellular compartments.

MPA-QDs To Determine pH in Live Cells. The results obtained with MPA-QDs deposited on glass slides suggested that these pH nanosensors could be promising pH nanosensors as intracellular probes with FLIM technology. This methodology is particularly attractive for intracellular sensing because of the advantages of time-resolved fluorescence techniques. Sensors based on emission intensity have several disadvantages for quantitative measurement because they are prone to be affected by concentration dependence, interference from cell autofluorescence, and several sources of optical excitation power drift. However, the use of PL decay times and FLIM may overcome many of these limitations. For example, in contrast to intensity measurements, PL lifetime is independent of the local concentration of the probe and is inherently robust in the presence of absorption and scattering, although it is still highly sensitive to changes in the environment. These advantages, combined with the excellent intrinsic optical properties of QDs, such as resistance to photobleaching and longer decay times, enable long-lasting cell tracking and monitoring of the intracellular environment for the detection of changes related to various processes.

Thus, these MPA-QD nanosensors were introduced into live cells to probe intracellular pH. First, MC3T3-E1 or CHO-k1 cells were seeded onto glass slides and incubated with MPA-QD solutions added to the culture medium for 2 h at 37 °C. Both CHO-k1 and MC3T3-E1 cells maintained their native morphology during and after incubation with QDs, indicating that the QD nanosensors had low toxicity, at least at the concentration range and the time frame of the experiments. After the incubation time, the cells internalized the nanoparticles, mainly by cellular endocytosis, and the cells were scanned to obtain confocal FLIM images. The effective incorporation of the QD nanoparticles into the cytoplasm was confirmed by the use of a lipophilic membrane dye. MC3T3-E1 cells were labeled with

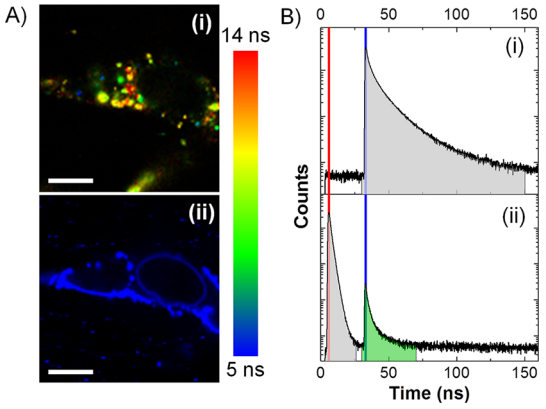

Figure 2. (A) FLIM images of MC3T3-E1 cells incubated with MPA-QDs and DiD membrane dye: QD detection channel (i) and DiD membrane dye detection channel (ii). The scale bars (white lines) represent 10 μm. (B) Overall PL decay traces from detection channels (i) and (ii) in (A). Gray shaded regions indicate the effective time window selected to rebuild the FLIM images in each channel. The red and blue lines indicate the times for the 635 and 470 nm laser pulses, respectively. The bleedthrough of the MPA-QD emission into the DiD detection channel, shaded in green, was effectively eliminated.

Vybrant DiD dye, which was excited by an interleaved 635 nm laser (see Experimental Section). This setup, with two different detection channels and two interleaved excitation lasers, permits the establishment of two different detection time windows for the 470 and 635 nm excitations, effectively eliminating bleedthrough[36,37] of the MPA-QD emission into the DiD detection channel (see Figure 2B). As shown in Figure 2A, the MPA-QD nanoparticles were localized in the cell interior within the same confocal plane as the cell membrane, indicating that the nanosensors were successfully incorporated into the cytoplasm.

The excellent features of the FLIM technique make the QD-based nanosensors particularly sensitive and selective because they can be easily distinguished from other interfering fluorescence, such as cellular autofluorescence. Figure 3A shows the FLIM images of MC3T3-E1 cells before and after incubation with MPA-QD nanoparticles. The cells shown in this figure were also incubated with the ionophore nigericin and buffers mimicking the extracellular medium at pH 4.87 (ii) and 8.14 (iii) to change the intracellular pH (see below and Experimental Section for more details). In the absence of QDs, the cells displayed minimal PL emission at the low laser power employed in the acquisition and an even distribution of autofluorescence lifetimes across the entire cell, with lifetimes ranging from 1.45 and 2.43 ns. This lifetime range of intrinsic cell autofluorescence is similar to the fluorescence lifetime of most conventional dyes (1−5 ns)[5] and is thus completely indiscernible based on emission lifetime. However, the FLIM images of cells after the uptake of MPA-QD showed a strong contrast between the QD lifetimes and autofluorescence (Figure 3A). The bright spots are

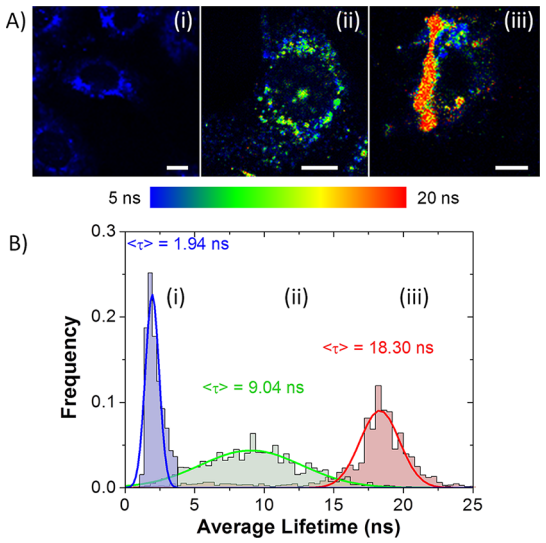

Figure 3. FLIM images (A) and lifetime distributions (B) of MC3T3-E1 cells before (i) and after incubation with MPA-QD (ii and iii). Image (i) shows the autofluorescence of the cells. MC3T3-E1 cells were incubated with nigericin and buffers mimicking the extracellular medium at pH 4.87 (ii) and 8.14 (iii). The scale bars (white lines) represent 10 μm.

QDs inside the cytosol, which were mostly incorporated *via* endocytosis. As indicated by the arbitrary color scale and the lifetime distributions in Figure 3A,B, the PL average lifetime associated with the QDs was significantly longer than that of cell autofluorescence, even when the pH on the inside of the cells was fairly acidic and the MPA-QD nanosensors displayed the shortest lifetimes. These long lifetimes are one of the main advantages of using QD nanoparticles as intracellular imaging probes because they facilitate the discrimination between the signal from the probe and the intrinsic fluorescence of the cells and produce an enhanced signal-to-background ratio.

Many intracellular fluorescence microscopy studies emphasize the need for fluorophores in the red or near-infrared region of the spectrum to avoid the contribution of green cell autofluorescence.[38,39] However, we have demonstrated that the use of FLIM eliminates the requirement for a near-infrared probe. The CdSe/ZnS QDs employed in this work exhibited green fluorescence with an emission maximum centered at 535 nm,[8] within the range of the green autofluorescence of cells. Nevertheless, FLIM overcomes the spectral limitation of the fluorescent probe as long as the fluorescence lifetime of the dye is noticeably longer than that of the cell autofluorescence.

Once the excellent advantages of the combination of FLIM with QDs for intracellular detection were established, the usefulness of the MPA-QDs for intracellular sensing and pH determination was evaluated in the cytoplasm of CHO-k1 cells. To further explore the effect of changes in the intracellular pH on the PL lifetime of MPA-QDs in these cells, the pH of the cell medium was varied from 4.70 to 8.2 by exposing the

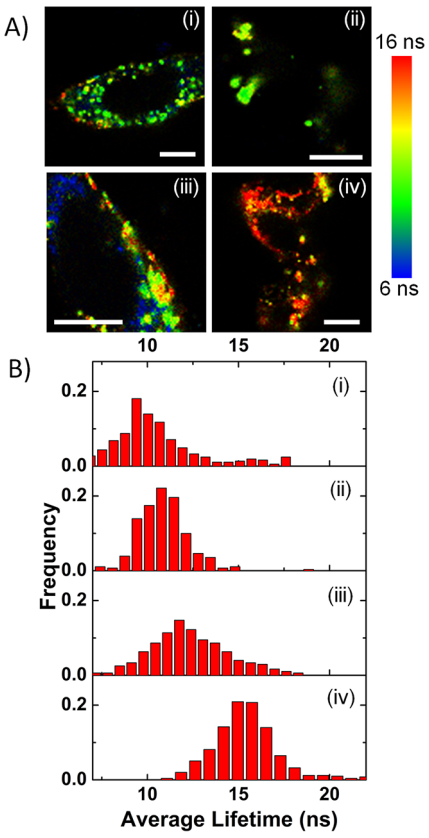

Figure 4. FLIM images (A) and recovered lifetime histograms (B) of MPA-QDs in the cytoplasm of CHO-k1 cells after incubation with nigericin in extracellular buffers (EBs) at different pH values: 5.70 (i), 6.50 (ii), 6.73 (iii), and 8.19 (iv). The scale bars (white lines) represent 10 μm.

cells to the H^+/K^+ ionophore nigericin. The extracellular buffers (EB) contained K^+ at the intracellular concentration but at different pH values. The ionophore nigericin equilibrates the concentration of H^+ and K^+ along the cellular membrane. When the extracellular K^+ concentration is similar to the intracellular K^+ concentration in the presence of nigericin, the intracellular pH approximates the extracellular value.[40] In these experiments, the EBs, which provide the depolarizing concentration of extracellular K^+, were prepared to reach different pH values by mixing different proportions of the following solutions: (a) 135 mM KH_2PO_4 + 20 mM NaCl and (b) 110 mM K_2HPO_4 + 20 mM NaCl. After the uptake of the QD nanoparticles, the cells were incubated in the EBs at 37 °C for 10 min and were scanned to record the FLIM images.

Figure 4 shows the changes in the PL lifetime of MPA-QDs in the cytoplasm of CHO-k1 cells treated with nigericin in EBs at pH values of 5.70, 6.50, 6.73, and 8.19. The arbitrary color scale of the FLIM images permits the direct visualization of the changes in the MPA-QD emission lifetime. Likewise, the PL lifetime distributions of the regions of interest (pixels with QD emission detected) permit a more quantitative recognition. The PL decays of MPA-QDs in the cellular cytoplasm

displayed the typical temporal behavior of these nanoparticles, indicating that the cytosolic environment does not significantly affect the multiexponential kinetics of these semiconductor nanoparticles. However, the PL decays were fitted to three exponentials because the number of photons collected from the images of the QDs in the cells was lower than that obtained when the QDs were suspended on glass slides. Further optimization of the laser power or the scanning speed could increase the number of photons collected. Figure S3 in the Supporting Information shows a larger compilation of representative FLIM images and PL lifetime distributions, demonstrating the reproducibility of the results.

These results suggest the excellent response of the proposed MPA-QD lifetime-based nanosensors inside the cells. When the MPA-QD nanosensors are compared with other well-settled intracellular pH indicators, the advantages of the proposed methodology are still well-evidenced. For instance, BCECF has been the most widely used pH indicator for intracellular sensing by ratiometric excitation methods but is unsuitable in ratiometric emission approaches since its relative emissions at any two different wavelengths are not significantly dependent on pH.[41] However, unlike our method, BCECF shows disadvantages for intracellular pH measurements, such as pK_a shifting from 7.8 to 6.8 depending on the ionic strength of the environment[42] and leakage from cells.[43] Furthermore, if the dye accumulates in certain regions of the cell, then it can provide different pH values indicative of dye concentration differences. Ratiometric cell permeant benzoxanthene dyes, such as the SNARF family, have also been widely used.[41] These compounds show improved properties as pH indicators because their ratiometric fluorescence is not significantly dependent on the dye's concentration or on the ionic strength of the surrounding aqueous media, but they also show some drawbacks, such as low quantum yields and the fact that intracellular pH values under 7.0 cannot be measured accurately because of a pK_a as high as 7.5.[44] Giving that certified standards for measuring intracellular pH do not exist, the advantages of our method should support a performance at least as reliable as the well-established approaches. Moreover, our sensor also presents the previously mentioned advantages of the FLIM technique over other intracellular fluorescent nanoparticle-based pH sensors that use PL intensity as the detection signal.[23,34,40,45,46] Only a few studies have investigated the combination of pH-sensitive QDs and PL lifetime measurements, with no reports on intracellular applications.[8,10,34] For instance, Mattoussi and colleagues developed a QD−dopamine bioconjugate that included the characterization of the pH response with lifetime measurements. Nevertheless, for monitoring variations in the intracellular pH, they did not take advantage of the time-resolved techniques but used conventional fluorescence microscopy.[34] Another benefit of the proposed methodology is that it only needs a single detection channel, in contrast with the ratiometric approaches, which require multicolor or multichannel detection systems.[45,46] Thus, to the best of our knowledge, this work represents the first attempt to detect and quantify changes in the intracellular pH with lifetime imaging of QD nanoparticles in living cells. This application demonstrates the advantages of the FLIM methodology, particularly in combination with QD nanoparticles, whose very long PL lifetime greatly enhances the sensitivity and selectivity of the nanosensors.

CONCLUSIONS

We have demonstrated the unique features of FLIM in combination with QD nanoparticles for intracellular sensing. Although previous studies have reported nanosensors based on modified QDs, luminescence intensity has been by far the most popular choice for the detection, mainly because they require relatively inexpensive instruments and simpler performance and analysis. In this work, it has been shown that PL lifetime is highly sensitive to changes in the environment, which permits its use as detection signal for the development of sensors. As a proof of principle, the intracellular pH was monitored using pH-sensitive MPA-QDs and time-resolved fluorescence methodologies. The FLIM technology permits the monitoring of pH changes within the cellular cytoplasm and therefore provides a sensitive readout for the quantification of the intracellular pH.

The results presented herein show a successful first approach. Nevertheless, there is still a place for several improvements. On the one hand, automation of the analysis process can shorten the postprocessing time. Although an intensity threshold was employed to ensure the analysis of pixels containing only QDs emission, a visual inspection of the selected regions of the image was required to avoid potential artifacts. The development of automated algorithms for the selection of regions of interest is, hence, an attractive line for progress. On the other hand, the linear response of the proposed nanosensors is located around 6.0−7.5, which limits their applications to this range. However, the applications might be extended to the quantification of the pH in other cellular compartments with more acidic pHs, like endosomes and lysosomes, by the correct modification of the QD surface. For instance, we are currently optimizing the attachment of some specific receptor groups on the QDs in order to deliver the nanosensors to particular organelles, like the mitochondria. This would permit measuring changes of pH within these compartments during important cellular processes. In addition, we are also investigating the effect of active charge transfer derivatives attached on the QD surface to cause shifts to the pH response.

With careful selection of the chemistry on the QD surface for the preparation of new nanoscale, intracellular sensitive probes, the method can be extended to the determination of a wide range of molecules with high biological impact inside cells. Thus, FLIM is a useful tool on which to base the development of new time-resolved-based nanosensors for use in research.

EXPERIMENTAL SECTION

Materials. All experiments were performed using molecular biology grade chemicals and Milli-Q water. CdSe/ZnS core–shell QDs with a maximum emission at 535 nm and hexadecylamine as a lipophilic chain surfactant were purchased from Evident Technologies (New York, NY). 3-Mercaptopropionic acid (MPA) was purchased from Fluka (Spain). Ficoll400, bovine serum albumin (BSA), nigericin, and all inorganic salts and buffers were used as obtained from Sigma-Aldrich (Spain). The pH of solutions and buffers was adjusted using diluted NaOH and HCl dissolved in Milli-Q water. Vybrant DiD membrane cell labeling solution was purchased from Invitrogen (Spain). For cell culture, Dulbecco's modified Eagle's medium (DMEM), alpha minimum essential medium (αMEM), fetal bovine serum (FBS), penicillin, and streptomycin were obtained from Sigma. All chemicals were used as received without further purification, and stock solutions were kept at 4 °C in a refrigerator and in the dark when not in use to avoid possible deterioration *via* exposure to light and heat. All solutions were filtered with 0.2 μm filters (Whatman) before use.

Synthesis of Water-Soluble MPA-Capped CdSe/ZnS Nanoparticles. As reported previously,[3] core–shell QDs coated with MPA (MPA-QDs) were obtained by exchange of the lipophilic (hexadecylamine, HDA) capping on the surface of the commercial CdSe/ZnS core/shell QDs with a water-soluble molecule, MPA. The procedure is briefly described in the Supporting Information. These nanoparticles were stable for several months, provided that they were kept dissolved in buffer solutions of pH greater than 7. At acidic pH, the MPA-QD nanoparticles started to aggregate. The final concentration of the nanoparticles was calculated by absorption spectroscopy.

Cell Culture. Wild-type Chinese hamster ovary (CHO-k1; ATCC No. CCL-61) and MC3T3-E1 preosteoblast (ECACC 99072810) cell lines were provided by the Cell Culture Facility, University of Granada. CHO-k1 cells were grown in DMEM supplemented with 10% (v/v) FBS, 2 mM glutamine, 100 U/mL penicillin, and 0.1 μg/mL streptomycin at 37 °C in a humidified 5% CO_2 incubator. MC3T3-E1 cells were grown in αMEM containing 10% fetal bovine serum and 1% penicillin–streptomycin at 37 °C in a humidified 5% CO_2 incubator, as described previously.[47] For the microscopy experiments, CHO-k1 and MC3T3-E1 cells were seeded onto 20 mm diameter slides at a density of 11 250 cells/cm^2. The glass slides were washed with DMEM medium and phosphate-buffered saline (PBS) before adding the cells.

QD Uptake and Intracellular pH Modification with Nigericin. CHO-k1 and MC3T3-E1 cells seeded onto glass slides were incubated with MPA-QDs (200 μL, 2 μM in Tris pH 8) for 2 h at 37 °C. The cells were washed twice with 10 mM Tris buffer at pH 7.4. The QD-loaded cells were later incubated at 37 °C for 10 min with a buffer mimicking the extracellular medium (extracellular buffers, EB) in the presence of 5.2 μM nigericin, a H^+/K^+ ionophore.[40] The EB was prepared by mixing appropriate proportions of solutions of 135 mM KH_2PO_4/20 mM NaCl and 110 mM K_2HPO_4/20 mM NaCl at room temperature to obtain different pH values ranging from 4.70 to 8.16.

Instrumentation. Fluorescence lifetime images were recorded with a MicroTime 200 fluorescence lifetime microscope system (PicoQuant, GmbH, Germany) using the time-tagged time-resolved (TTTR) methodology, which permits the reconstruction of the photoluminescence decay traces from the QD nanoparticles in the confocal volume. In the experiments involving solely QDs in a single detection channel, the excitation source consisted of a 440 nm pulsed laser (LDH-P-C-440, PicoQuant GmbH, Germany), operating at a power of ~0.9 μW. The experiments performed with QDs in cell cultures with Vybrant DiD as the cell membrane reporter were carried out in the same instrument, but using dual-color pulsed interleaved excitation (PIE).[36,37] The excitation was achieved by two spatially overlapped lasers, alternated on the nanosecond time scale. The two lasers were a 470 nm (LDH-P-C-470, PicoQuant) and a 635 nm (LDH-P-635, PicoQuant) pulsed laser. Further details on the FLIM setup can be found in the Supporting Information. In all experiments, data acquisition was performed with a Timeharp 200 single photon timing module (PicoQuant) in TTTR mode, with a time resolution of 116 ps per channel, enabling the reconstruction of the PL decay histogram. To image a region, the sample was raster-scanned with an $x-y$ piezo-driven device. The image data were normally acquired with a 512 × 512 pixel resolution with a collection time of 0.60 ms per pixel.

Photoluminescence decay traces of the QDs in bulk solutions mimicking the intracellular environment were recorded in single photon timing mode using the FluoTime 200 fluorometer (PicoQuant, GmbH) described previously.[7] Briefly, the samples were excited by the 440 nm pulsed laser mentioned above with a 10 MHz repetition rate. The full width at half-maximum of the laser pulse was ~80 ps. The fluorescence was collected after crossing through a polarizer set at the magic angle and a 2 nm bandwidth monochromator. Fluorescence decay histograms were collected in triplicate using a TimeHarp200 board with a time increment per channel of 36 ps at an emission wavelength of 540 nm, until reaching 6 × 10^4 counts in the peak channel. The histograms of the instrument response function (IRF) were acquired with a LUDOX scatterer.

FLIM Imaging of MPA-QDs in Buffered Solutions and in CHO-k1 and MC3T3-E1 Cells. FLIM imaging experiments of MPA-QDs at different pH values were performed in 10 mM Tris buffer or in buffer solutions mimicking the intracellular environment. The composition of these synthetic intracellular buffers (SIB) was 10 mM Tris buffer, 150 mM K^+, 50 mM Na^+, 1 mM Ca^{2+}, 1 mM Mg^{2+}, 1% Ficoll400, and 0.2 mg·mL^{-1} BSA, adjusted to different pH values with HCl or NaOH. The following protocol was used for image acquisition. The microscope glass slide was washed and sonicated twice with 1 M KOH, followed by ethanol. Once the slide was positioned on the microscope objective, the surface was washed twice with 40 μL of the buffer to be analyzed. Then, 40 μL of the MPA-QDs (approximately 400 nM) was dissolved in the same buffer at the required pH and was deposited on the slide. After 5 min, the solution was removed, and an additional 40 μL of the buffer was added. This protocol ensured that the coating of the surface was not too crowded, was suitable for imaging, and avoided interactions between individual nanoparticles, while maintaining the pH of the solution. Finally, raster-scanned confocal images in TTTR mode were recorded by the MicroTime 200 fluorescence lifetime microscope system. A prescan of a wide area was performed to choose regions of interest. Then, smaller regions (between 100 and 300 μm^2) were imaged with a spatial resolution of 20 to 35 nm/pixel.

For the microscopy experiments with CHO-k1 and MC3T3-E1 cells, the glass slides with seeded cells loaded with MPA-QDs were imaged on the FLIM microscope. Unless otherwise stated, 80 × 80 μm regions were scanned with a spatial resolution of 156 nm/pixel.

Methods of Analysis. The FLIM image data were analyzed using SymphoTime (PicoQuant) software. The FLIM images were reconstructed by sorting all photons corresponding to a single pixel into a temporal histogram by the TTTR methodology. The regions of interest (pixels containing QD emission and at least 200 photons per pixel) were selected, and the overall PL decay trace from these regions was reconstructed. The decay trace was fitted to a three- or four-exponential function through an iterative reconvolution method (see Supporting Information) based on the maximum likelihood estimator (MLE), which yields

the best parameter fitting for low count rates.[48] The instrument response function for the iterative reconvolution analysis was reconstructed from a monoexponential decay trace from 30 nM fluorescein in basic pH aqueous solution, using the SymphoTime software. To obtain the FLIM image, spatial rebinning of 5×5 pixels and temporal binning of four channels in the single photon timing scale (for a final 464 ps/channel temporal resolution) were employed to achieve higher counts in each pixel. The individual decay traces in each pixel were fitted to the same multiexponential function, leaving the decay times as fixed parameters and the pre-exponential factors as the only adjustable parameters. The image could then be redrawn using an arbitrary color scale showing the average lifetime values in each pixel, calculated using eq 1:[49]

$$\tau_{ave} = \sum a_i \tau_i^2 / \sum a_i \tau_i \quad (1)$$

In the images from the cell interior, a decay time of 1.5 ns was fixed to account for cell autofluorescence. The average decay time of the QDs was then calculated using eq 1 but removing the contribution of the 1.5 ns component.

Frequency distributions of the average lifetimes found in the pixels of interest are presented in Figures 1, 3, and 4. These distributions give an idea of the average lifetime value, as well as the precision of the measurements (width of the distributions). Broad distributions indicate a heterogeneous environment for the MPA-QDs. These distributions have the potential to reveal the presence of different populations (different pH environments). The single average PL lifetimes reported in Figure 1C and Figure S1 are the arithmetic mean from the average lifetimes in all the pixels in the regions of interest.

Conflict of Interest: The authors declare no competing financial interest.

Acknowledgment. This work was supported by Grant CTQ2010-20507/BQU from the Ministerio Español de Ciencia e Innovación (cofinanced by FEDER funds) and Grant GREIB PYR 2010-14 from the GREIB Startup project for young researchers. The authors also thank Dr. M. D. Giron and Dr. R. Salto for kindly supplying the cell cultures.

Supporting Information Available: Supporting experimental; FLIM data of Tris-buffer-suspended MPA-QDs on slides; PL decay traces and pH response of MPA-QDs in bulk solutions mimicking the cellular cytoplasm; and FLIM data of MPA-QDs in the cytoplasm of CHO-k1 cells at different pH values. This material is available free of charge *via* the Internet at http://pubs.acs.org.

REFERENCES AND NOTES

1. Alivisatos, A. P.; Gu, W.; Larabell, C. Quantum Dots as Cellular Probes. *Annu. Rev. Biomed. Eng.* **2005**, *7*, 55–76.
2. Ruedas-Rama, M. J.; Hall, E. A. H. Azamacrocycle Activated Quantum Dot for Zinc Ion Detection. *Anal. Chem.* **2008**, *80*, 8260–8268.
3. Ruedas-Rama, M. J.; Hall, E. A. H. A Quantum Dot-Lucigenin Probe for Cl^-. *Analyst* **2008**, *133*, 1556–1566.
4. Snee, P. T.; Somers, R. C.; Nair, G.; Zimmer, J. P.; Bawendi, M. G.; Nocera, D. G. A Ratiometric CdSe/ZnS Nanocrystal pH Sensor. *J. Am. Chem. Soc.* **2006**, *128*, 13320–13321.
5. Resch-Genger, U.; Grabolle, M.; Cavaliere-Jaricot, S.; Nitschke, R.; Nann, T. Quantum Dots *versus* Organic Dyes as Fluorescent Labels. *Nat. Methods* **2008**, *5*, 763–775.
6. Byrne, S. J.; Corr, S. A.; Rakovich, T. Y.; Gun'ko, Y. K.; Rakovich, Y. P.; Donegan, J. F.; Mitchell, S.; Volkov, Y. Optimisation of the Synthesis and Modification of CdTe Quantum Dots for Enhanced Live Cell Imaging. *J. Mater. Chem.* **2006**, *16*, 2896–2902.
7. Ruedas-Rama, M. J.; Orte, A.; Hall, E. A. H.; Alvarez-Pez, J. M.; Talavera, E. M. Effect of Surface Modification on Semiconductor Nanocrystal Fluorescence Lifetime. *ChemPhysChem* **2011**, *12*, 919–929.
8. Ruedas-Rama, M. J.; Orte, A.; Hall, E. A. H.; Alvarez-Pez, J. M.; Talavera, E. M. Quantum Dot Photoluminescence Lifetime-Based pH Nanosensor. *Chem. Commun.* **2011**, *47*, 2898–2900.
9. Ruedas-Rama, M. J.; Orte, A.; Hall, E. A. H.; Alvarez-Pez, J. M.; Talavera, E. M. A Chloride Ion Nanosensor for Time-Resolved Fluorimetry and Fluorescence Lifetime Imaging. *Analyst* **2012**, *137*, 1500–1508.
10. Tang, R.; Lee, H.; Achilefu, S. Induction of pH Sensitivity on the Fluorescence Lifetime of Quantum Dots by NIR Fluorescent Dyes. *J. Am. Chem. Soc.* **2012**, *134*, 4545–4548.
11. Jens, U. S.; David, J. S. B.; Olaf, J. R. CdSe/ZnS Core/Shell Quantum Dots as Luminescence Lifetime Sensors for Cu^{2+}. *Meas. Sci. Technol.* **2012**, *23*, 055103.
12. Esposito, A.; Gralle, M.; Dani, M. A. C.; Lange, D.; Wouters, F. S. pHlameleons: A Family of FRET-Based Protein Sensors for Quantitative pH Imaging. *Biochemistry* **2008**, *47*, 13115–13126.
13. Tantama, M.; Hung, Y. P.; Yellen, G. Imaging Intracellular pH in Live Cells with a Genetically Encoded Red Fluorescent Protein Sensor. *J. Am. Chem. Soc.* **2011**, *133*, 10034–10037.
14. Harvey, C. D.; Ehrhardt, A. G.; Cellurale, C.; Zhong, H.; Yasuda, R.; Davis, R. J.; Svoboda, K. A Genetically Encoded Fluorescent Sensor of ERK Activity. *Proc. Natl. Acad. Sci. U.S.A.* **2008**, *105*, 19264–19269.
15. Kuimova, M. K.; Yahioglu, G.; Levitt, J. A.; Suhling, K. Molecular Rotor Measures Viscosity of Live Cells *via* Fluorescence Lifetime Imaging. *J. Am. Chem. Soc.* **2008**, *130*, 6672–6673.
16. Paredes, J. M.; Girón, M. D.; Ruedas-Rama, M. J.; Orte, A.; Crovetto, L.; Talavera, E. M.; Salto, R.; Alvarez-Pez, J. M. Real-Time Phosphate Sensing in Living Cells Using Fluorescence Lifetime Imaging Microscopy (FLIM). *J. Phys. Chem. B* **2013**, 10.1021/jp405041c.
17. Zhang, Y.; Birch, D. J. S.; Chen, Y. Two-Photon Excited Surface Plasmon Enhanced Energy Transfer between DAPI and Gold Nanoparticles: Opportunities in Intra-cellular Imaging and Sensing. *Appl. Phys. Lett.* **2011**, *99*, 103701-3.
18. Dahan, M.; Laurence, T.; Pinaud, F.; Chemla, D. S.; Alivisatos, A. P.; Sauer, M.; Weiss, S. Time-Gated Biological Imaging by Use of Colloidal Quantum Dots. *Opt. Lett.* **2001**, *26*, 825–827.
19. Giraud, G.; Schulze, H.; Bachmann, T.; Campbell, C.; Mount, A.; Ghazal, P.; Khondoker, M.; Ross, A.; Ember, S.; Ciani, I.; *et al.* Fluorescence Lifetime Imaging of Quantum Dot Labeled DNA Microarrays. *Int. J. Mol. Sci.* **2009**, *10*, 1930–1941.
20. Pai, R. K.; Cotlet, M. Highly Stable, Water-Soluble, Intrinsic Fluorescent Hybrid Scaffolds for Imaging and Biosensing. *J. Phys. Chem. B* **2011**, *115*, 1674–1681.
21. Carlini, L.; Nadeau, J. L. Uptake and Processing of Semiconductor Quantum Dots in Living Cells Studied by Fluorescence Lifetime Imaging Microscopy (FLIM). *Chem. Commun.* **2013**, *49*, 1714–1716.
22. Conroy, J.; Byrne, S. J.; Gun'ko, Y. K.; Rakovich, Y. P.; Donegan, J. F.; Davies, A.; Kelleher, D.; Volkov, Y. CdTe Nanoparticles Display Tropism to Core Histones and Histone-Rich Cell Organelles. *Small* **2008**, *4*, 2006–2015.
23. Liu, Y.-S.; Sun, Y.; Vernier, P. T.; Liang, C.-H.; Chong, S. Y. C.; Gundersen, M. A. pH-Sensitive Photoluminescence of CdSe/ZnSe/ZnS Quantum Dots in Human Ovarian Cancer Cells. *J. Phys. Chem. C* **2007**, *111*, 2872–2878.
24. Susha, A. S.; Javier, A. M.; Parak, W. J.; Rogach, A. L. Luminescent CdTe Nanocrystals as Ion Probes and pH Sensors in Aqueous Solutions. *Colloids Surf., A* **2006**, *281*, 40–43.
25. Gao, X.; Chan, W. C. W.; Nie, S. Quantum-Dot Nanocrystals for Ultrasensitive Biological Labeling and Multicolor Optical Encoding. *J. Biomed. Opt.* **2002**, *7*, 532–537.
26. Wang, X.; Boschetti, C.; Ruedas-Rama, M. J.; Tunnacliffe, A.; Hall, E. A. H. Ratiometric pH-Dot ANSors. *Analyst* **2010**, *135*, 1585–1591.
27. Jiang, X.; Weise, S.; Hafner, M.; Röcker, C.; Zhang, F.; Parak, W. J.; Nienhaus, G. U. Quantitative Analysis of the Protein Corona on FePt Nanoparticles Formed by Transferrin Binding. *J. R. Soc. Interface* **2010**, *7*, S5–S13.

28. Maffre, P.; Nienhaus, K.; Amin, F.; Parak, W. J.; Nienhaus, G. U. Characterization of Protein Adsorption onto FePt Nanoparticles Using Dual-Focus Fluorescence Correlation Spectroscopy. *Beilstein J. Nanotechnol.* **2011**, *2*, 374–383.
29. Carlheinz, R.; Matthias, P.; Feng, Z.; Wolfgang, J. P.; Nienhaus, G. U. A Quantitative Fluorescence Study of Protein Monolayer Formation on Colloidal Nanoparticles. *Nat. Nanotechnol.* **2009**, *4*, 577–580.
30. Warnement, M. R.; Tomlinson, I. D.; Chang, J. C.; Schreuder, M. A.; Luckabaugh, C. M.; Rosenthal, S. J. Controlling the Reactivity of Ampiphilic Quantum Dots in Biological Assays through Hydrophobic Assembly of Custom PEG Derivatives. *Bioconjugate Chem.* **2008**, *19*, 1404–1413.
31. Liu, W.; Howarth, M.; Greytak, A. B.; Zheng, Y.; Nocera, D. G.; Ting, A. Y.; Bawendi, M. G. Compact Biocompatible Quantum Dots Functionalized for Cellular Imaging. *J. Am. Chem. Soc.* **2008**, *130*, 1274–1284.
32. Bawendi, M. G.; Carroll, P. J.; Wilson, W. L.; Brus, L. E. Luminescence Properties of CdSe Quantum Crystallites: Resonance between Interior and Surface Localized States. *J. Chem. Phys.* **1992**, *96*, 946–954.
33. Hille, C.; Berg, M.; Bressel, L.; Munzke, D.; Primus, P.; Löhmannsröben, H.-G.; Dosche, C. Time-Domain Fluorescence Lifetime Imaging for Intracellular pH Sensing in Living Tissues. *Anal. Bioanal. Chem.* **2008**, *391*, 1871–1879.
34. Medintz, I. L.; Stewart, M. H.; Trammell, S. A.; Susumu, K.; Delehanty, J. B.; Mei, B. C.; Melinger, J. S.; Blanco-Canosa, J. B.; Dawson, P. E.; Mattoussi, H. Quantum-Dot/Dopamine Bioconjugates Function as Redox Coupled Assemblies for *In Vitro* and Intracellular pH Sensing. *Nat. Mater.* **2010**, *9*, 676–684.
35. Despa, S.; Steels, P.; Ameloot, M. Fluorescence Lifetime Microscopy of the Sodium Indicator Sodium-Binding Benzofuran Isophthalate in HeLa Cells. *Anal. Biochem.* **2000**, *280*, 227–241.
36. Müller, B. K.; Zaychikov, E.; Bräuchle, C.; Lamb, D. C. Pulsed Interleaved Excitation. *Biophys. J.* **2005**, *89*, 3508–3522.
37. Kudryavtsev, V.; Sikor, M.; Kalinin, S.; Mokranjac, D.; Seidel, C. A. M.; Lamb, D. C. Combining MFD and PIE for Accurate Single-Pair Förster Resonance Energy Transfer Measurements. *ChemPhysChem* **2012**, *13*, 1060–1078.
38. Terpetschnig, E.; Wolfbeis, O. S. Luminescent Probes for NIR Sensing Applications. In *Near-Infrared Dyes for High Technology Applications*; Daehne, S., Resch-Genger, U., Wolfbeis, O., Eds.; Springer: Berlin, 1998; Vol. 52, pp 161−182.
39. Buschmann, V.; Weston, K. D.; Sauer, M. Spectroscopic Study and Evaluation of Red-Absorbing Fluorescent Dyes. *Bioconjugate Chem.* **2002**, *14*, 195–204.
40. Peng, J.; He, X.; Wang, K.; Tan, W.; Wang, Y.; Liu, Y. Noninvasive Monitoring of Intracellular pH Change Induced by Drug Stimulation Using Silica Nanoparticle Sensors. *Anal. Bioanal. Chem.* **2007**, *388*, 645–654.
41. Han, J.; Burgess, K. Fluorescent Indicators for Intracellular pH. *Chem. Rev.* **2009**, *110*, 2709–2728.
42. Boens, N.; Qin, W.; Basarić, N.; Orte, A.; Talavera, E. M.; Alvarez-Pez, J. M. Photophysics of the Fluorescent pH Indicator BCECF. *J. Phys. Chem. A* **2006**, *110*, 9334–9343.
43. Rink, T. J.; Tsien, R. Y.; Pozzan, T. Cytoplasmic pH and Free Mg^{2+} in Lymphocytes. *J. Cell Biol.* **1982**, *95*, 189–196.
44. Balut, C.; vandeVen, M.; Despa, S.; Lambrichts, I.; Ameloot, M.; Steels, P.; Smets, I. Measurement of Cytosolic and Mitochondrial pH in Living Cells during Reversible Metabolic Inhibition. *Kidney Int.* **2008**, *73*, 226–232.
45. Shi, W.; Li, X.; Ma, H. A Tunable Ratiometric pH Sensor Based on Carbon Nanodots for the Quantitative Measurement of the Intracellular pH of Whole Cells. *Angew. Chem., Int. Ed.* **2012**, *51*, 6432–6435.
46. Dennis, A. M.; Rhee, W. J.; Sotto, D.; Dublin, S. N.; Bao, G. Quantum Dot−Fluorescent Protein FRET Probes for Sensing Intracellular pH. *ACS Nano* **2012**, *6*, 2917–2924.
47. Ito, M.; Haito, S.; Furumoto, M.; Uehata, Y.; Sakurai, A.; Segawa, H.; Tatsumi, S.; Kuwahata, M.; Miyamoto, K.-i. Unique Uptake and Efflux Systems of Inorganic Phosphate in Osteoclast-like Cells. *Am. J. Physiol. Cell Physiol.* **2007**, *292*, C526–C534.
48. Maus, M.; Cotlet, M.; Hofkens, J.; Gensch, T.; De Schryver, F. C.; Schaffer, J.; Seidel, C. A. M. An Experimental Comparison of the Maximum Likelihood Estimation and Nonlinear Least-Squares Fluorescence Lifetime Analysis of Single Molecules. *Anal. Chem.* **2001**, *73*, 2078–2086.
49. Lakowicz, J. R. *Principles of Fluorescence Spectroscopy*, 3rd ed.; Springer: Berlin, 2006.